


Review

Non-Circular Cross-Section Fibres for Composite Reinforcement—A Review with a Focus on Flat Glass Fibres

James Thomason ^{*}, Andrew Carlin and Liu Yang 

Department of Mechanical and Aerospace Engineering, University of Strathclyde, 75 Montrose Street, Glasgow G1 1XJ, UK; a.carlin@strath.ac.uk (A.C.); l.yang@strath.ac.uk (L.Y.)

* Correspondence: james.thomason@strath.ac.uk

Abstract: Glass fibre reinforcements form the backbone of the composites industry. Today, glass fibre products account for more than 95% of the fibre reinforcements used in the composites industry. Since the first commercialisation of glass fibres for composite reinforcement in the 1930s, the cross-sectional shape of glass fibres has remained exclusively circular. However, many of the other types of fibre reinforcement have a non-circular cross section (NCCS). This paper reviews the available knowledge on the production of NCCS glass fibres and some of the possibilities that such fibres offer to enhance the performance of glass reinforced polymer composites. The three parts of the review focus on early research work on different shapes of glass fibre, the developments leading to industrial-level production of NCCS glass fibres, and the more recent data available on the influence of the available commercially produced NCCS flat glass fibres on composite performance. It is concluded that the continued development of NCCS glass fibres may offer interesting potential to generate composites with increased performance and may also enable further tailoring of composite performance to enable new applications to be developed.

Keywords: glass fibre; flat fibre; cross-section; composites; reinforcement



Citation: Thomason, J.; Carlin, A.; Yang, L. Non-Circular Cross-Section Fibres for Composite Reinforcement—A Review with a Focus on Flat Glass Fibres. *Fibers* **2024**, *12*, 98. <https://doi.org/10.3390/fib12110098>

Academic Editor: Constantin Chaliotis

Received: 25 September 2024
Revised: 4 November 2024
Accepted: 6 November 2024
Published: 11 November 2024



Copyright: © 2024 by the authors. Licensee MDPI, Basel, Switzerland. This article is an open access article distributed under the terms and conditions of the Creative Commons Attribution (CC BY) license (<https://creativecommons.org/licenses/by/4.0/>).

1. Introduction

Glass fibre reinforced composites (GFRPs) are utilised extensively across a range of sectors due to competitive price and performance-to-weight ratio. While glass is an ancient material, the mass production of glass fibre is a relatively new development, widely agreed to have begun in the 1930s with developments at Owens Corning [1]. Glass fibre use is widespread in the composites industry due to its highly attractive performance-to-price ratio. Despite this relatively long history of glass fibre usage and multiple developments in the glass and sizing formulation, the cross-section (CS) geometry of the glass fibres used in nearly all applications has remained exclusively circular.

However, recently, there have been a number of developments from glass fibre manufacturers in the production of non-circular cross-section (NCCS) glass fibres [2–4]. Furthermore, it is well known that many of the carbon fibres on the market do not have circular cross-sections [5], and the more recent upsurge in interest in the use of natural fibres as a composite reinforcement also brings many different and variable fibre cross sections into the available reinforcement portfolio [6,7]. Hence, NCCS glass fibres are now commercially available, and in fact, other NCCS fibres have been used in many composite applications for some time.

Consequently, it is of interest to consider whether a change in the CS shape of glass fibre offers an opportunity to improve fibre and composite performance. The continuing global growth of composite material usage comes in part from an attractive performance-to-weight ratio but also from the ability of a composite material to be tailored to its application. Changing the cross-sectional shape further expands the ‘tailorability’ of this glass fibre reinforced polymer (GFRP) composite, thus the useful properties and potential applications. Such a change has resulted in improvements in other reinforcement and functional

fibres in a broad range of applications. Within the field of GFRPs, such a change remains relatively unexplored.

This paper reviews the available literature on NCCS GFRPs to explore the potential of NCCS glass fibre to affect single fibre properties, the level of interfacial stress in composite materials, and the performance of composites at a macroscopic level. The review focusses, in particular, on the recently commercially available flat-shaped glass fibres but covers other glass fibre shapes and, where appropriate, the effects of non-circularity of fibre cross section in other fibre reinforcements. The three parts of the review will focus on early experimental work on different CS shapes of glass fibre, the developments leading to industrial-level production of NCCS glass fibres, and the more recent data available on the influence of the available commercially produced NCCS glass fibres on potential composite performance.

2. Early NCCS Fibre Investigations

2.1. Ribbons

Much of the early experimental work published on the use of NCCS glass fibres focussed on ribbon (microtape) reinforcement or shaped single glass fibres produced on drawing towers similar to those being developed for the optical fibre industry. Ribbons can possess certain advantages over circular CS (CCS) fibres insofar as they are theoretically capable of providing substantial biaxial reinforcement in a polymer composite. In addition to reinforcement along its longitudinal axis, a ribbon may provide reinforcement in the plane parallel to its flat surface. Halpin and Thomas published an analysis of the potential of ribbon-shaped reinforcement in composite materials applications [8]. They used a micromechanical analysis approach to show that ribbon reinforcement delivers higher in-plane stiffness performance in a composite lamina. Figure 1, based on the equations in their paper, shows the ratio of transverse stiffness for a unidirectional (UD) glass–epoxy composite based on NCCS rectangular ribbon fibres versus CCS fibres for different ribbon cross-section aspect ratios and different fibre volume fractions. It can be seen that at high ribbon aspect ratios, the composite transverse stiffness is predicted to be enhanced by up to 200% in the in-plane direction, with a loss of approximately 40% in the out-of-plane direction.

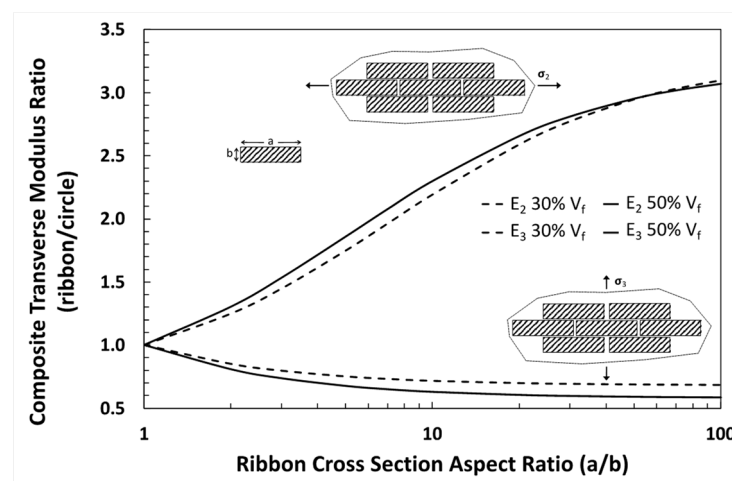


Figure 1. Predicted transverse modulus ratio of UD epoxy composites with ribbon and circle-shaped glass fibres [8].

Lim presented a more complex analytical model to estimate the transverse modulus of aligned NCCS ribbon-reinforced composites [9]. Values for the model input parameters were based on E-glass and epoxy polymer. The results of the model were not dissimilar to those of Halpin and Thomas in that the transverse in-plane modulus of the composite was predicted to be significantly increased across all fibre volume fractions, from that of a CCS fibre reinforcement, as the aspect ratio of the ribbon increased. This coincided with a much

smaller percentage decrease in out-of-plane transverse modulus. The author concluded that NCCS ribbon-reinforced composites are advantageous over conventional unidirectional CCS fibre composites, especially in the application of very thin laminas.

Brydges et al. presented a theoretical, analytical study of the fluid permeability of glass ribbon-reinforced organic matrix composites [10]. Their analysis indicated that such composites, with ribbon aspect ratios in the range of 50 to 200, offer two to three orders of magnitude improvement in permeation resistance over CCS fibreglass composites. Permeation characteristics of glass ribbon epoxy composites, made by hand lay-up, were also determined experimentally using mass spectrograph measurements of helium penetration. The authors claimed that the experimental results qualitatively agreed with the predictions of the analytical model. Gulati reported longitudinal and transverse strength measurements of an NCCS glass ribbon with a rectangular cross section measuring $5.6 \text{ mm} \times 50 \text{ }\mu\text{m}$ [11]. It was found that in the as-manufactured condition, the transverse strength of the ribbon is lower than the longitudinal strength, indicating a preferred orientation of flaws introduced during manufacturing. Strength in both directions could be increased by surface etching after which the transverse strength was reported as generally higher than the longitudinal strength.

Li and Weng modelled the creep performance of glass–epoxy composites reinforced with NCCS randomly oriented elliptic fibres [12]. Along all loading directions, the ribbon-reinforced composite was consistently predicted to exhibit the strongest creep resistance, and as the aspect ratio (width/thickness) decreases, the creep resistance also continues to lessen, with the circular fibres (aspect ratio = 1) providing the poorest reinforcement in terms of creep resistance. In a similar paper, the same authors also modelled the strain-rate sensitivity and stress–strain curves of the same composites and again predicted that the higher aspect ratio elliptical cross-section fibres were more effective than traditional circular fibres [13]. They suggested that there should be a move away from traditional circular CS fibres to NCCS elliptical fibre and, if at all possible, to thin ribbons in order to optimise composite strength.

Rexer and Anderson presented a review of composite with planar reinforcements, such as ribbons [14]. They also showed that if these ribbons are arranged parallel to the principal plane in composites, then they provide superior performance to CCS fibre reinforcements under two-dimensional loading conditions. Improvements in the modulus of a factor three and in the tensile strength of a factor two were shown to be possible. Another potential advantage listed by these authors was that planar reinforcements should allow the manufacture of composites with higher reinforcement volume fractions than CCS fibres, and this could lead to higher technical performances. This could include increased resistance to liquid or vapour penetration due to the long path length through the composite imposed by the impermeable planar reinforcements. The authors commented that, despite these potential advantages, composites using planar reinforcements were still relatively unknown. It was proposed this situation could be due to the fact that such planar reinforcements were not readily available and consequently were little researched. It may be commented that this situation is still reasonably valid forty-plus years later.

2.2. NASA Funded Research

During the 1960s, NASA issued a number of contractor reports on the properties of NCGFs and their composites. In one of these, Rosin and Hashin presented experimental data which showed that 4:1 aspect ratio NCCS elliptical fibres properly packed in 50% volume fraction composites have a transverse stiffness in the major axis direction of the ellipses which was 80% higher than that of CCS fibre reinforced composites [15]. In this case, the experimental data were obtained on composites produced using aluminium inclusions in epoxy resin. In another NASA report by Eakins and Humphrey, the feasibility of producing NCCS glass fibres was demonstrated using a method of drawing single fibres [16]. It was first necessary to fabricate an elongated glass preform with a cross section approaching that of the desired fibre. The drawing process used a mechanical device for

feeding a shaped preform into a furnace with a tailored vertical temperature gradient, along with a winder whose speed was coordinated with that of the feeder. The report contains a Table describing the production conditions for over 60 different fibre shapes, along with micrographs of their cross sections. Although many of these NCCS fibres were about one order of magnitude greater in size than the commonly used commercial glass fibres, there were some samples of comparable dimensions range (a solid ellipse cross section of $16 \times 64 \mu\text{m}$ and a flat microtape of $12 \mu\text{m}$ thickness). Humphrey also reported the use of this drawing method to produce NCCS hexagonal E-glass filaments measuring $18 \mu\text{m}$ across flats [17]. The drawn fibre was then coated with an aminosilane coupling agent, sprayed with a low viscosity epoxy resin, and then filament wound on a mandrel. However, there were issues of devitrification of the E-glass, and consequently, the tensile strength of the fibres was low (345 MPa).

In the following report, Humphrey discussed the filament winding (FIWI) manufacture of composite materials using some of the NCCS glass fibres from a previous report [18]. NCCS glass fibres were drawn as previously described [16], and resin (usually epoxy) was applied directly just above the puller/winder. The resin-wetted fibre is then drawn onto a rotating reciprocating mandrel to form a composite tube (after appropriate curing). Precision windings were made to obtain close packing from rectangular microtape with a $12 \times 500 \mu\text{m}$ cross section. The tube dimensions were 58 mm internal diameter, 1 mm wall thickness and length 0.75 m with a glass content of 90%. Such high glass content cannot be achieved by FIWI of CCS fibre composites. It was reported that these high glass content composites displayed no room temperature permeability to water and modulus values at 70 GPa, the same as the glass. The axial strengths of the tubes with only circumferential windings were as high as 175 MPa.

Another NASA report describes further development and characterisation of FIWI composite tubes made with glass microtape reinforced epoxy resin. In this report, a slightly larger NCCS microtape of $38 \times 1500 \mu\text{m}$ was used [19]. It was noted that the use of borosilicate glass was abandoned because of its tendency to devitrify and thereby lose strength at the forming temperatures used in the preform-drawing process. Consequently, soda-lime window glass was used throughout the research program. The average tensile strength measured on drawn CCS $10 \mu\text{m}$ diameter glass fibres was 2.36 GPa. In contrast, two much lower values were reported for NCCS glass microtapes. An average tensile strength of 0.81 GPa was found for a $12.5 \times 380 \mu\text{m}$ cross-section sample and 1.27 GPa for a $10.5 \times 365 \mu\text{m}$ cross-section sample. Another development in this report was the addition of a silane coupling agent in the resin mix applied to the microtape during the FIWI process. Once again, a striking feature of the test results on the FIWI composites was the unusually high modulus demonstrated by the high glass (90% by weight) content tubes. Additional to the NASA reports, Humphrey also published a short book chapter summarising some of the main results of this extensive research project [20]. It was proposed that the remarkably high modulus values obtained on the precision wound glass microtape composites could be due to their thin, flat resin matrix layers combined with the large overlap of the individual microtape fibres leading to a more monolithic glass structure instead of a composite. It was stated that NCCS glass fibres have the potential for producing composites with advantages in performance, including the following:

- Low bulk density, permeability, dielectric constant and matrix content;
- High stiffness- and strength-to-weight ratios and high transparency;
- Anisotropic properties to meet specific design requirements.

2.3. Other Fibre Cross-Section Shapes

Dow presented an analytical solution to determine the effect of NCCS triangular glass fibres on epoxy composite transverse stiffness [21]. The ratio of transverse stiffness of triangular fibres to that of CCS fibres is shown in Figure 2 as a function of fibre volume fraction. It was stated that one characteristic of these equilateral triangular fibres is that the composite transverse stiffness is enhanced in both transverse directions. It was suggested

that this isotropy through the composite thickness may be advantageous in applications in which multiaxial stresses are encountered. It was also shown that NCCS elliptical fibres also gave improved composite transverse stiffness.

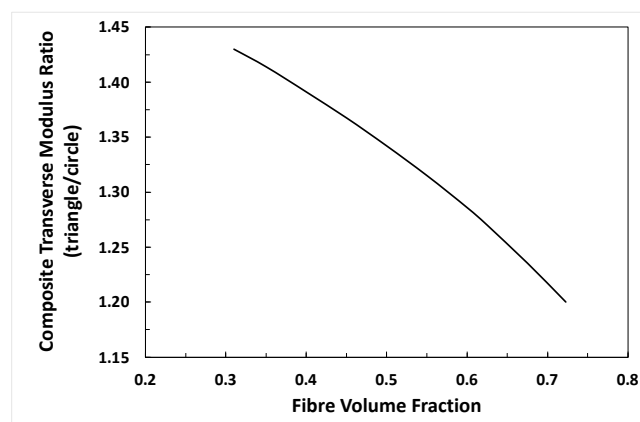


Figure 2. Predicted transverse modulus ratio of UD epoxy composites with triangle and circle-shaped glass fibres [21].

Bond et al. also reported on the mechanical performance of circular and NCCS triangular glass fibres and their composites (see Figure 3) [22]. Continuous single glass fibre was produced by drawing from alumino-borosilicate glass rod preforms using a modified optical fibre manufacturing apparatus. The fibres were approximately equal in CS area (equivalent to 45 μm diameter), which was significantly greater than the typical commercial glass fibres used in composite reinforcement. Unlike the fibre used in early work by Humphrey [16–18], these fibres were also coated with sizing to reduce surface damage, maintain fibre strength, and improve interfacial compatibility with polymer matrices. The fibres were processed with epoxy resin into UD composites using a pre-pregging method followed by film stacking and autoclave curing. Interestingly, micro-composite compression testing revealed that NCCS triangular fibres recorded a 60% higher compressive strength compared to CCS fibres, and this was reflected in triangular fibre composites with a 40% higher compression strength. Single fibre testing indicated that the NCCS triangular fibres had a significantly higher (+26%) average tensile strength despite having a 28% greater surface area (which could, therefore, have more strength, lowering surface flaws). This was also reflected in higher (+16%) tensile strength in triangular fibre reinforced composites. Despite the higher surface area of the triangular fibres, their composites only showed a slightly higher (but not statistically significant) interlaminar shear strength (ILSS). Robati and Attar modelled the response of composite materials, UD reinforced with NCCS triangular and CCS glass fibres in the presence of a pin load hole using both numerical and analytical methods [23]. The results showed that values of compressive stress developed in the fibres behind the pin were about 28% less in NCCS triangular fibre laminates. The maximum tensile stresses were also shown to be about 17% less in these samples.

Liu et al. investigated the performance of filament-wound triangle-shaped carbon fibre reinforced epoxy composites with approximately 50 vol.% fibre content [24]. The flexural strength and modulus were found to be 20% and 13% higher, respectively, compared to that of CCS carbon fibre composites. The authors attributed the higher performance of the NCCS fibres to their higher surface:volume ratio, which effectively lowered interfacial stress levels. The authors stated that the tensile strength and modulus of the two types of composites were equivalent, although no data were presented to support that claim. A later paper, which apparently used the two composites, investigated composite transverse properties both experimentally and using finite element analysis [25]. Both the experimental data and the modelling results appeared to show little or no significant difference in the transverse tensile modulus and strength and the compressive strength between the NCCS and CCS fibre composites.

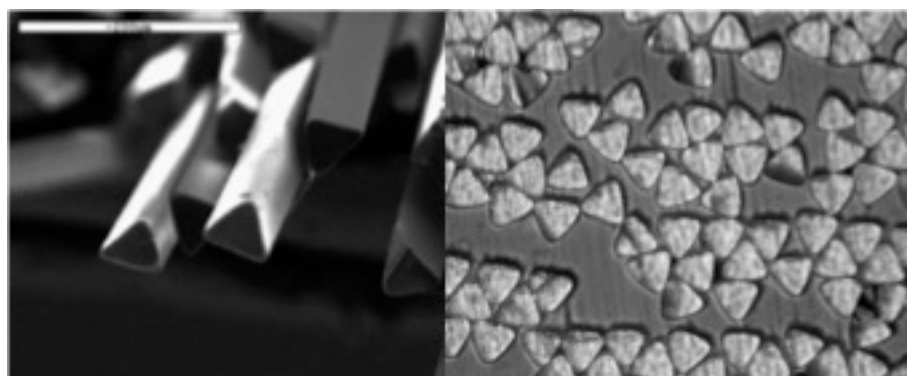


Figure 3. (Left) SEM micrographs of 50 μm triangular glass fibres, (right) optical micrograph cross section through unidirectional 60 μm triangular glass fibre composite ($V_f \sim 50\%$) [22].

Gallucci et al. briefly reported on the properties of injection-moulded NCCS glass fibre reinforced PBT [26]. The bi-lobal and tri-lobal glass fibres used were experimental samples prepared by Owens Corning fibreglass [27,28] with a cross-sectional area equivalent to a 10 μm diameter CCS glass fibre. They reported a reduction in the composite warpage of 30% to 40% when using bi-lobal glass fibres in comparison to circular fibres. In contrast, the tri-lobal fibres gave composite performance similar to round fibres and were not significantly effective in reducing composite warp. Further analysis showed only small variations in other mechanical properties, no significant differences in residual fibre length, and no major differences in fibre orientation.

Harris et al. published a discussion paper on the use of NCCS fibres to improve the through-thickness properties of composites [29]. Twelve qualitative guidelines for the geometry of novel-shaped reinforcing fibres were described, and the bounds they place on fibre designs are discussed. The paper concluded with a proposal for a fibre design, a six-lobed geometry (see Figure 4), which conformed to most of the suggested guidelines. In a second paper, the same authors produced such NCCS borosilicate glass fibres using the fibre drawing tower described by Bond et al. [22] and used the same pre-pregging method to produce UD epoxy laminates [30]. The six-lobed fibres had an average outer diameter of 50 μm , whereas circular fibres with the same CS area had a diameter of 42 μm . Composites were prepared, and Mode I double cantilever beam (DCB) testing indicated that the NCCS multi-lobed fibres provided more than 50% improvement in strain energy release rate (G_{Ic}) over circular fibres.

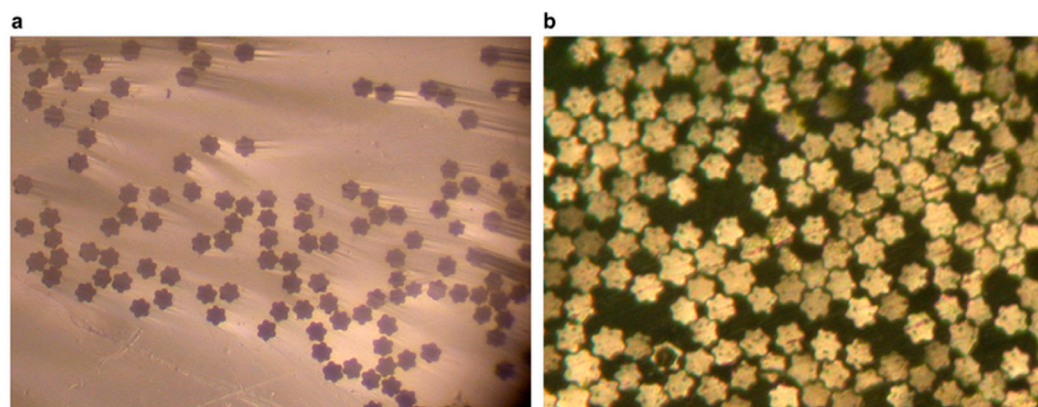


Figure 4. (a) Six-lobed shaped glass fibres with an outermost diameter of 50 μm and (b) a transverse section through an epoxy composite plate of the same fibres [29].

Agnese and Scarpa recently published a series of papers describing numerical and experimental comparisons of CCS and NCCS star-shaped (four-lobed) fibres for vibration damping in wind turbine blades [31–33]. Their finite element simulations revealed a

significant dependence of the strain energy distribution within a composite to the fibre shape. The results showed that changing the geometry of the fibres from CCS to NCCS star-shaped increased the strain energy in the viscoelastic area by 30%. This increase was also recorded experimentally using a novel shear test rig to detect the dynamic properties of aluminium-epoxy composites.

Yang et al. used finite element modelling to study the effect of gear-shape (multi-lobed) fibres on the transverse mechanical properties of unidirectional composites [34]. They compared NCCS fibres with 12, 16 and 20 lobes with CCS fibre reinforced composite. Their simulation results showed that the NCCS fibre composites all had a predicted higher transverse stiffness and strength than the CCS composites. There were two possible hypotheses proposed to explain this effect. Firstly, the gear-shaped fibres possess a much higher surface area and can, therefore, provide a greater interfacial bond. Secondly, propagation of interfacial debonds and matrix cracking is made more resisted by the more complex boundary geometry of the gear-shaped fibres.

Recent efforts by the carbon fibre industry to produce more cost-effective carbon fibres have resulted in the commercialisation of carbon fibres with irregular CS, often denoted as kidney-bean shaped fibres [35–37]. Although there is, as yet, no sign of such a CS shape in glass fibres, there has been considerable research activity, both experimental and modelling, expended on this shape of fibre. Xu et al. have shown that kidney-shaped fibres have a larger specific surface area and, consequently, better adsorption characteristics and higher surface free energy compared with circular fibres [38]. Single fibre microbond testing of interfacial strength and short beam shear testing of interlaminar shear strength showed that the NCCS kidney-type fibre/epoxy composites outperformed the CCS composites by a significant margin of 23.5% and 12.7%, respectively. In a further report investigating the same materials, it was reported that the composites containing the NCCS kidney-shaped fibres exhibited a 7.5% higher flexural strength compared to the CCS fibres. No significant differences were found in tensile and compressive strengths [39]. It was of interest to note that the CS of the “circular” fibres in these studies were clearly far from being perfect circles (see Figure 5).

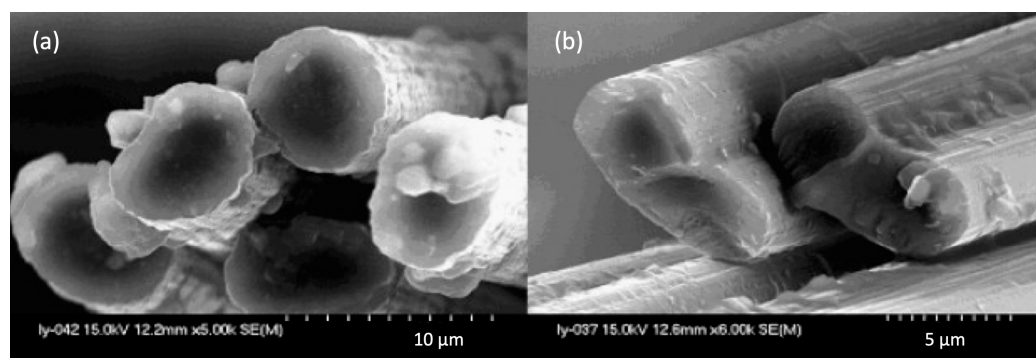


Figure 5. SEM micrographs of (a) circular carbon fibre and (b) kidney-bean shaped carbon fibre [38].

Hanhan and Sangid used finite element simulations to compare longitudinal stress distributions in NCCS kidney-bean shaped and CCS carbon fibre composites [37]. The results showed that at 1.5% strain, the NCCS microstructure reached simulated failure at approximately 2100 MPa, while the CCS microstructure did not fail at this strain level. A single fibre model showed that this was due to the curvature of the NCCS fibres inducing matrix stress that was 7 MPa higher compared to the CCS microstructure. Clarke et al. discussed the results of a computational study of the effect of fibre CS shape on the compressive strength of unidirectional carbon fibre epoxy composites [40]. It was predicted that at low fibre misalignment angles, NCCS kidney-shaped fibres exhibit higher composite compressive strength compared to CCS fibres. However, at larger misalignment angles, the compressive strengths of the different fibre shapes converge.

Reichanadter and Manson used flow simulations to model the transverse permeability of NCCS kidney-bean shaped fibres [36]. The maximum packing fraction for NCCS kidney-bean fibres was predicted to be 0.923, which is significantly larger than 0.907 for CCS fibres. The modelling predicted that the NCCS kidney-bean shaped fibres had up to 74% reduction in permeability. It was further predicted that the lower permeability resulted in the infiltration time of UD-packed NCCS fibres being significantly longer than similarly packed CCS fibres. This increase in infiltration time increased with fibre volume fraction (V_f) from about +50% at $V_f = 0.3$ up to +280% at $V_f = 0.75$. The same authors also reported an experimental evaluation of the compaction behaviour of NCCS kidney-bean shaped fibres [35]. The pressure–fibre volume fraction relationship for the kidney-bean fibres was shown to follow a different compaction trend compared to the circular fibres. The data showed that the kidney-shaped fibres required significantly more pressure to compact to an equal volume fraction. Kitagawa et al. presented results from an experimental and FEM modelling study of the effects of kidney-shaped carbon fibre on transverse cracking in epoxy UD laminates [41]. It was experimentally and numerically demonstrated that the NCCS kidney-shaped fibres suppress transverse crack build-up and retard crack initiation in CF-reinforced laminates when compared with CCS fibres.

2.4. Modelling Multiple Cross-Section Shapes

Higuchi et al. used a combination of an extended finite element method, a homogenisation method, and a Monte Carlo method to model the effects of the five fibre CS shapes (circular, elliptical, two-lobed, triangular, and square) on the macroscopic composite properties [42]. The modelling was based on a 40% volume fraction carbon fibre reinforced composite. The results predicted that, for UD composites with a random arrangement of CS shapes, the NCCS square fibres exhibited a 5% higher transverse (both directions) moduli. Interestingly, when the fibre CS shapes were arranged on a regular square array, the elliptical and bi-lobal fibres were predicted to exhibit a 24% and 18% higher in-plane transverse modulus, respectively, compared to CCS fibres. Camarena et al. used a micromechanical model to study the longitudinal compressive strength of composites containing a range of theoretical NCCS carbon fibres [43]. The results predicted that six-lobe fibres may improve strength between 10% and 13%, and the tri-lobe can give 6% to 9% stronger composites than circular fibres. Bi-lobal fibres did not show any significant improvement in compressive strength.

Wang and Hang used FEM modelling to study the effect of fibre CS shape on the transverse moisture diffusivities of their UD composites [44]. The study included a large range of NCCS fibre shapes. The conclusion was that fibre shape greatly influences the transverse diffusivity of UD composite with NCCS fibres randomly spaced and oriented (in the transverse plane). It was predicted that the transverse diffusivity decreased with the increase in the number of lobes around the fibre CS. He et al. investigated the effect of fibre CS shape on the strengths and failure mechanisms of UD composites by computational micromechanics [45]. The modelling input parameters were based on carbon fibre reinforced epoxy. A comparison was made between CCS fibres and NCCS elliptical fibres with a major-to-minor axis ratio of approximately three. The modelling predicted that the elliptical fibres improved the transverse tensile, compressive, shear strengths and longitudinal shear strength all by approximately 10%. From a modelling viewpoint, this result was obtained because a random distribution of elliptical fibres inhibited crack propagation, which allowed the UD representative volume element of the material to tolerate higher loadings.

3. Industrial Development of NCCS Glass Fibre Products

It will become apparent in the following discussion that the NCCS glass fibres which have reached a mass production stage are based on relatively simple CS shapes. There does not yet appear to be any major production of multi-lobal glass fibres. The CS of the glass fibres which are being mass-produced appear to be variations in “flat”, ribbon-type fibres

(rectangular, flat, and cocoon) with a major:minor axis ratio ($a:b$) in the range 2:1 to 5:1. This is illustrated in Figure 6. Rectangular-shaped fibres (with filleted edges) and elliptical (also called oval)-shaped fibres are both commonly referred to as flat. When considering flat fibres, it is also important to address the term flatness, also known as aspect ratio, flatness degree (or ratio), dimension ratio or slenderness (ratio). From this point onwards in the text, the ratio between the major axis (a) and the minor axis (b) will be known as flatness.

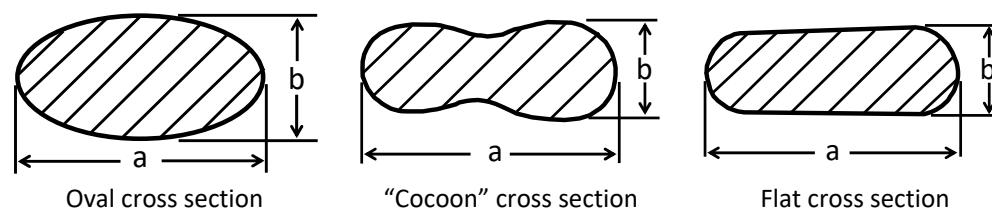


Figure 6. Typical cross-section shape of mass-produced commercial NCCS glass fibres.

From the foregoing review of the early work on NCCS glass fibres, it would appear that such fibres offer some considerable advantages in composite performance over normal CCS fibres. Indeed, Li and Weng, in their 1997 paper, suggested that there should be a move away from traditional circular CS fibres to NCCS elliptical fibre [13]. It might, therefore, be reasonable to question why, 25 years later and more than 50 years since the first papers on NCCS glass fibres were published, there still does not appear to be any major use of such fibres in structural composite applications. Clearly, any significant commitment to the use of NCCS glass fibres first requires that the production process for such fibres is scaled up from the single fibre drawing process used in many of the examples reviewed above. To better understand the challenges involved in that step requires some understanding of the process and economics of industrial glass fibre production.

Nearly all reinforcement glass fibres are made by a direct draw process using glass melt, which is continuously fed from a large furnace. These furnaces are generally divided into three distinct sections, as shown in Figure 7 (temperatures are typical for E-glass processing) [46]. The premixed raw material (batch) is delivered into the furnace section for melting and homogenisation. The melt then flows into the refining section where the temperature is slightly lower, and then flows under gravity along a number of heated channels, the forehearth, to be delivered to the forming area. Here, the melt is distributed to a number of platinum alloy bushing plates which contain a geometric array of from 200 to as many as 8000 individual tipped outlets of 1–3 mm diameter [47]. As shown in Figure 8, the molten glass flows down through the bushing tips under the force of gravity and is then drawn down rapidly to produce continuous filaments, usually in the diameter range of 8–24 μm [48].

Due to the relatively low value of glass fibre products (in comparison to other reinforcements) and the high fixed and variable costs of manufacture (the furnace and associated infrastructure and energy requirements), the profit margins in glass fibre manufacturing are relatively low. Consequently, maintaining a high process conversion efficiency is critical to achieving an acceptable cost of manufacture and profitability. One of the major issues in maintaining conversion efficiency is the occurrence of fibre breaks in the forming process [47,49]. A single fibre break under the bushing will generally lead to the failure of the entire bushing position, which then needs to be manually stabilised and restarted by an operator. The restart of the bushing position, from breakout to producing in-spec product, can take several minutes during which the glass flow cannot be stopped and is therefore wasting glass. A large quantity of costly glass melt, which can amount to up to 15–20% of the total production, is thus lost [47–51].

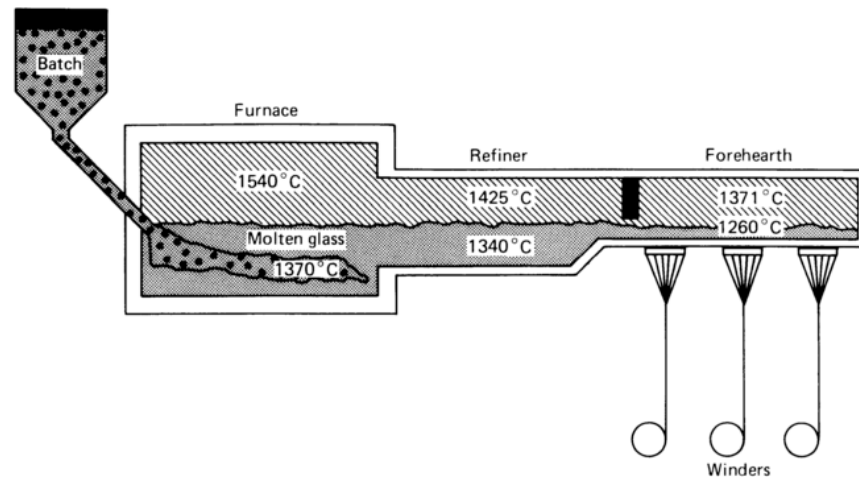


Figure 7. Typical furnace for glass melting in glass fibre production [46].

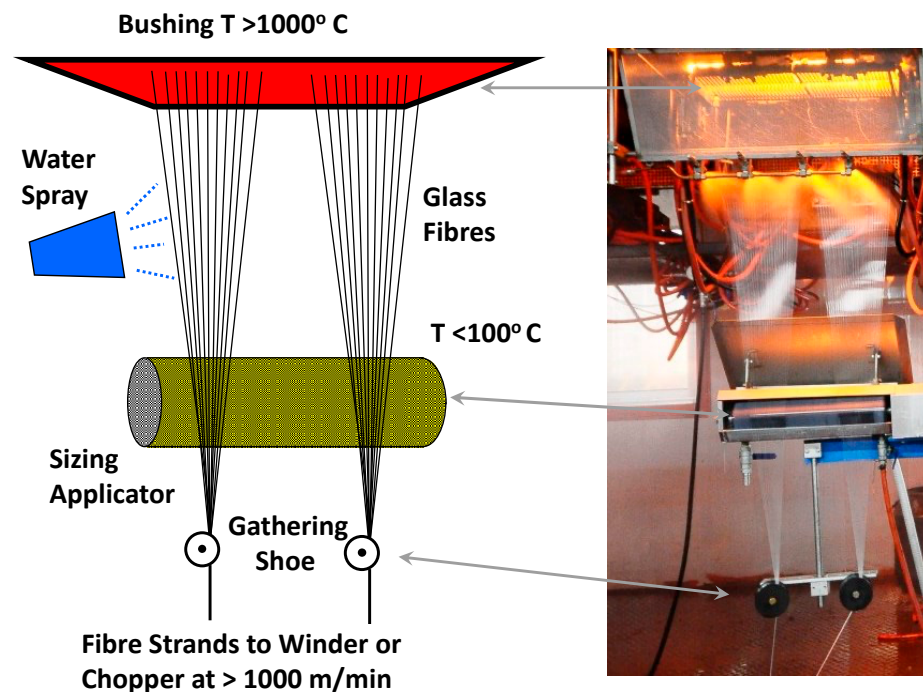


Figure 8. Schematic and picture of a glass fibre-forming position [48].

Besides costs caused by the material loss, there is also a further cost incurred due to the need to dispose of this waste. Chouffart studied the break rate of a commercial glass fibre production operation, recording the average daily break rate over 40 forming positions [50]. The results shown in Figure 9 are expressed in the number of breaks per bushing operating hours (B/BOH). The recorded break rate averaged over the entire year was 0.71 B/BOH, which would result in an active production efficiency of 94% and about 600 kg per hour of glass waste was being produced for that furnace. Clearly then, any alteration to the forming process which might decrease fibre spinnability and increase the average break rate is highly undesirable to the fibre manufacturer. In the review of the early literature on NCCS glass fibres, it was already noted that working with E-glass was more challenging for fibre drawing than some other glass formulations. However, E-glass is the standard formulation for most reinforcement glass fibres, so it can be considered most improbable that a manufacturer would consider changing a furnace glass formulation for a new product development. Hence, it seems quite likely that the not-insignificant challenges of obtaining a stable platform for the mass production of NCCS E-glass fibres have played

a role in the slow development of NCCS glass products. This may well have also been compounded by a general lack of demand from the composite industry for such products.

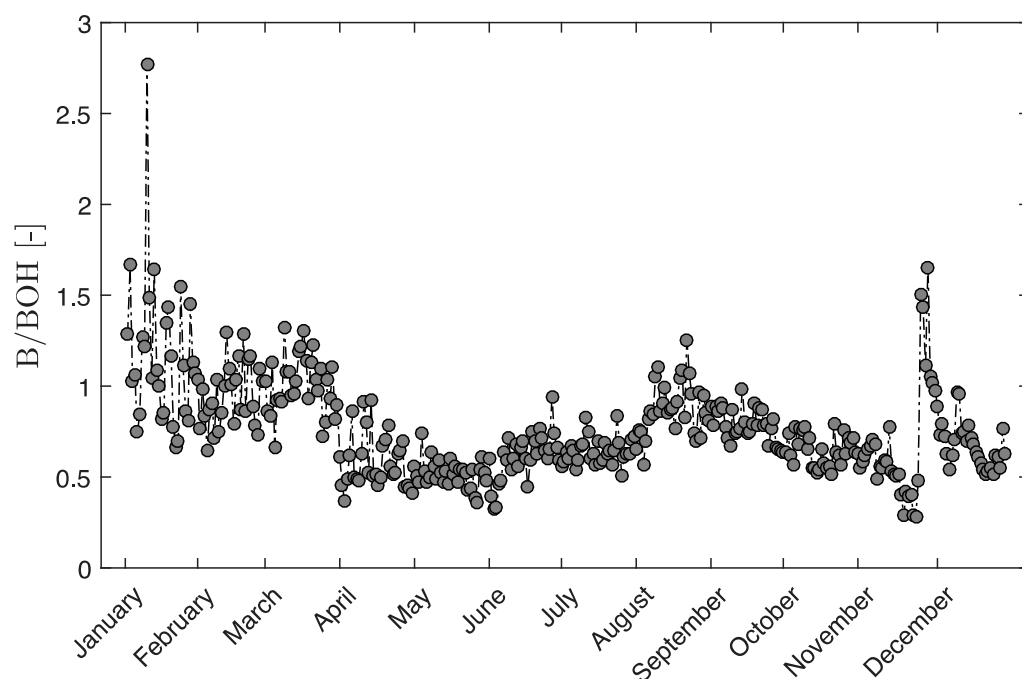


Figure 9. Daily fibre break rate averaged over ~40 bushings expressed in the number of breaks per bushing operating hours [50].

Nevertheless, as mentioned in the Introduction, there are currently at least three major glass fibre suppliers who have undertaken to tackle these challenges and have developed NCCS glass fibre products [2–4]. The patent literature gives some insight into how this has been accomplished and also currently serves as a limited source of information on the performance of composites produced with such mass-produced NCCS glass fibres. A short list, which should not be considered exhaustive, of patents from the four companies who appear to have been most active in these developments is available in the Supplementary Material. Given that manufacturers are unlikely to change their glass formulation to improve the spinnability of NCCS fibres, the focus of these developments has been on the fibre-forming part of the process and, in particular, on the bushing.

Yue has recently discussed the parameters governing glass fibre spinnability (the ability to continuously produce fibre without breaks) in the production glass fibre-forming environment [52]. Fibre forming is sensitive to the intrinsic parameters of the glass melt (such as surface tension, viscosity, and crystallisation temperature) and also to the extrinsic parameters of the process (such as draw speed, melt flow rate, cooling conditions, and nozzle geometry). The intrinsic parameters are determined by melt chemistry, which, for this discussion, is fixed as that of E-glass, whereas the extrinsic ones are dependent on the design of the process. One challenge to the mass production of NCCS glass fibres is the high surface tension (250–300 mN/m) of glass melts [53]. As a result of this, even with a bushing tip having a non-round CS, the effect of surface tension tends to force the melt into a round cross section once it has exited the tip. An interesting example of this phenomenon is found in a patent from PPG Industries Inc., which describes bushing plates where the tips have a non-circular CS, and yet the design is for the production of CCS glass fibres [54,55]. Consequently, for the production of NCCS glass fibres, it is necessary to oppose this surface tension-driven tendency by rapidly increasing the viscosity of the forming NCCS-shaped melt as it is drawn down to the desired CS dimensions.

Literature suggests that the spinnability of glass fibres can be empirically estimated by the ratio of the melt viscosity to the melt surface tension [52]. The higher this ratio

is then the higher the spinnability. Figure 10 compares the temperature dependence of the melt viscosity and melt surface tension of boron free E-glass based on the data of Chouffart [49,50]. The values have been normalised to the values at 1268 °C. It can be seen that the variation in surface tension over the temperature range shown is two orders of magnitude less than that of the melt viscosity. Hence, the more influential factor controlling spinnability is the melt viscosity. In two 1985 patents from Owens Corning, Huey states that the lower viscosity and higher surface tension of glass make it about 100 times more difficult to prevent shaped glass fibres from changing back into glass fibres having circular cross sections [27,28]. The patent further discusses the use of rapid air quenching under the bushing to ensure the retention of an NCCS glass fibre shape. Examples are shown of a bushing with tri-lobal orifices, but it states that the orifices and the resulting fibres can be of various shapes, such as, for example, cross-shaped, star-shaped, penta-lobal, octa-lobal or rectangular. Examples of NCCS glass fibre production are given using a single-hole bushing and a 20-hole bushing plate with tipless tri-lobal orifices (it seems likely that these were used in papers and patents of the time). Figure 11 shows the effect of increasing cooling air velocity on the retention of the original bushing orifice CS in the resulting NCCS glass fibres. It can be seen that the tri-lobal CS is well maintained at 30 m/s but that the CS shape is reverting to circular as the cooling air velocity is reduced. It is stated that the normal cooling air velocity used with air-quenched bushings at about 2 to 4 m/s is an order of magnitude slower.

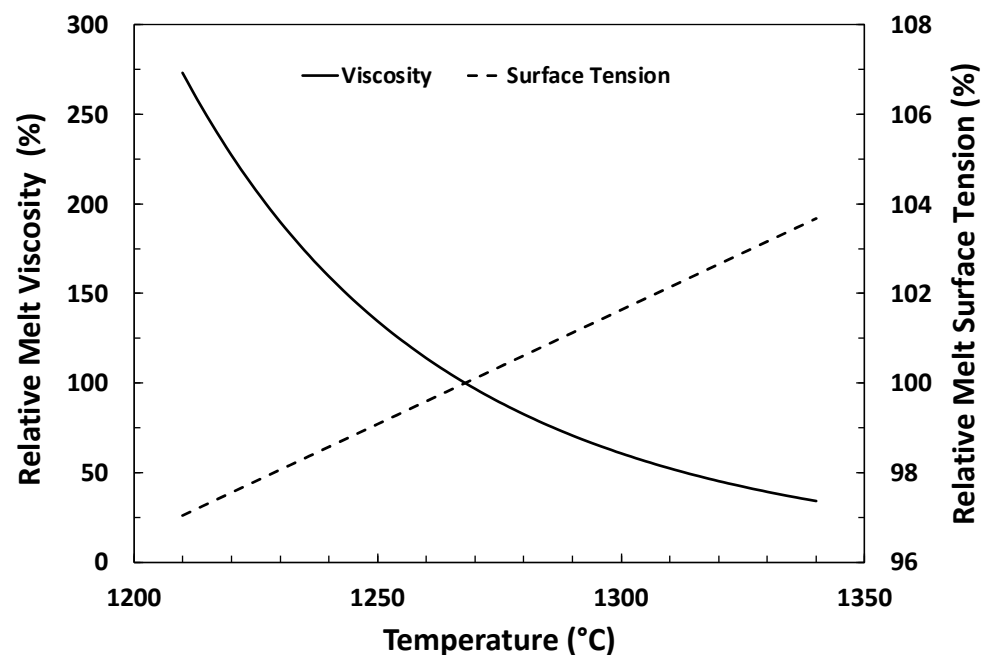


Figure 10. Temperature dependence of the relative viscosity and surface tension of an E-glass melt [49,50].

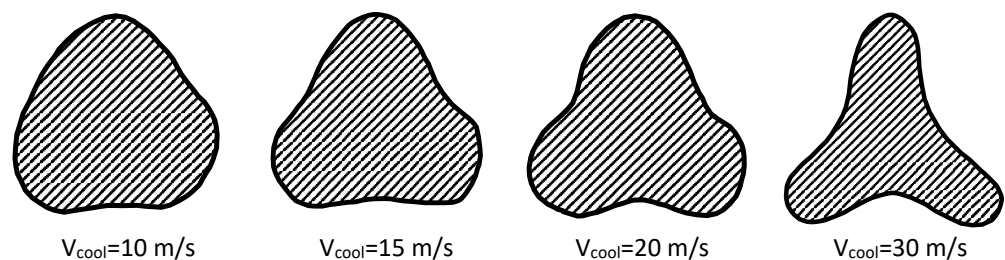


Figure 11. Effect of cooling air velocity (V_{cool}) on tri-lobal glass fibre shape (reproduced from [28]).

Owens Corning has also produced a number of other patents relating to the manufacture of NCCS glass fibres. As early as 1961, a patent describing a method to produce thin ribbons and other flat structures of NCCS directly by drawing from molten glass was filed [56]. One example claimed to draw a single flat glass ribbon 2 μm thick and eight to twelve times the width at 3 km/min. A 1977 patent disclosed a method for producing NCCS twisted filaments [57]. Owens Corning also has a number of patents on manufacturing hollowing glass fibres (which are not the subject of this review as they are circular in CS), and a variation on this method is found in a 1996 patent [58] which discloses a method of producing NCCS glass fibres by deforming hollow fibres under the bushing while they are still soft. Interestingly, although OC did manufacture and market hollow glass fibres for some years, there is no record to be found that they ever did so with NCCS glass fibre products. Nevertheless, a 1992 patent from Philips Petroleum Company claims the use of NCCS bi-lobal and tri-lobal glass fibres in composites [59]. The examples include a bi-lobal glass fibre (497DB-BF-02), a tri-lobal (497DB-TF-01) and a reference CCS fibre (497EE), all from Owens Corning and all with a CS area equivalent to a 9 μm diameter CCS fibre. The data in the examples reported on injection-moulded composites, 40 wt% fibre with a PPS matrix. The bi-lobal fibre composites exhibited improved flexural strengths (+8.5%), tensile strengths (+21%) and unnotched impact resistance (+23%) over the round and tri-lobal composites.

In contrast, the Japanese firm Nitto Boseki (commonly referred to as Nittobo) has an extensive patent portfolio related to NCCS glass fibres and also markets a range of NCCS glass fibre products [2], which was launched in 2006 [60]. One Nittobo patent filed in 1985 on the production of NCCS glass fibres discusses the need to lower the temperature to increase the glass melt's viscosity [61]. Since this also slightly lowers the surface tension, the theoretical spinnability is increased by both the change in viscosity and surface tension. The higher melt viscosity slows the rate of the solidifying melt cross section in its return to circularity. Consequently, it is stated that it is desirable that the temperature in the furnace is maintained at a comparatively low level. Another aspect of this patent is that it describes the design of bushing tips with multiple outlets which can initially form individual filaments which then coalesce to form an NCCS fibre. It also describes the importance of directed air-cooling jets to rapidly stabilise the fibre CS shape. The examples show an NCCS cocoon-shaped glass fibre. Later patents and literature using Nittobo fibres often refer to this cocoon CS, and their literature calls it an HIS-grade fibre [62,63]. It is stated in the patent (without supporting data) that these fibres produce higher bonding strength as compared with CCS glass fibres. It is suggested that this may be attributable to NCCS fibres having increased specific surface areas.

Another Nittobo patent filed in 1993 discusses a large range of potential bushing tip designs for manufacturing NCCS glass fibres [64]. There are many examples in the patent of different NCCS glass fibre shapes produced with E-glass on a 400-hole bushing at speed up to 3000 m/min (i.e., at conditions allowing mass production of such fibres). The key element of the new tip design is the addition of an extension downward of the tip on two small opposing sections of the tip circumference. This allows preferential cooling at the long axis sides of the fibre CS and helps stabilise the NCCS fibre shape. The inner part of the tip may be a simple single hole or may contain multiple orifices, potentially non-circular, similar to the design from the previously discussed patent [61]. A further 1997 patent from Nittobo claims another nozzle tip design which allows high-speed, stable (i.e., low B/BOH) spinning of highly flat glass fibres having a flatness ratio in the range of 2 to 10 [65]. Examples are given of NCCS glass fibres with flatness up to four produced on bushing with up to 256 fibres at a speed of up to 2000 m/min. Table S3 also contains a list of some of the patents in which Nittobo have described composite applications of flat fibres. Interestingly, these contain examples of composites with discontinuous flat fibre reinforcement but also examples with continuous fibre input, even though Nittobo does not currently appear to market continuous flat glass fibre products.

Chongqing Polycomp International Corporation (CPIC) and Nippon Electric Glass (NEG) also market a range of chopped NCCS glass fibre products. Both companies have also disclosed methods of manufacturing NCCS flat glass fibre in the patent literature (see Supplementary Material). CPIC flat fibre products have been available since around 2018 [4], and NEG launched their flat glass fibre product range in 2017 [3]. The patents of both companies also describe the requirements for flat fibre production along the lines already reviewed. These requirements mainly revolve around melt viscosity control, bushing tip design and increased fibre cooling to maintain a flat fibre CS shape.

The fact that none of these producers market continuous NCCS glass fibre products is not something that is discussed in the open literature. However, it is possible to hypothesise a number of possible explanations. There may, as yet, be little pull-through from the composite market for applications requiring such products, although there are certainly a number of patents on the use of continuous NCCS glass fibres in composite production (see Table S3). Another possible reason for the first available products being based on chopped glass fibres may have to do with the efficiency of the production process, especially with regard to waste. The use of continuous glass fibre reinforcement products in the composite industry makes extensive use of 20–25 kg bobbins of direct wound glass fibres. The production of such bobbins requires an uninterrupted run of fibres from any individual forming position of about 15–20 min. Hence, if a product experiences more frequent bushing breaks due to more challenging fibre-forming conditions, then not only is a higher level of waste produced during bushing downtime but also a high level of off-spec product (i.e., bobbins of <<20 kg weight). This is not the case for chopped glass fibre production, irrespective of whether the fibres are chopped in-line or off-line [47], since almost any weight of the bobbin can be used as input to a chopping process.

4. Performance of Composites Containing Commercial NCCS Flat Glass Fibres

It is notable that there are very few peer-reviewed research papers to be found on industrially produced NCCS glass fibres, and those that are available are focussed on injection-moulded composites, reflecting the previously mentioned fact that these are the only NCCS products which appear to have been commercialised so far. Consequently, much of the data reviewed in this section are taken from the fibre manufacturers' literature (mainly patents), which has not undergone peer review. Furthermore, it is also noted that in many of the referenced studies which compare the performance of composites containing flat and circular cross-section glass fibres, there is no discussion of whether the same sizing was applied to both types of fibre. It is certainly the case that if different sizings were used (for instance, when NCCS and CCS fibres came from different manufacturers), then differences in fibre–matrix adhesion and composite performance could be expected [47,48].

Deng and Mai reported on an early study of two types of NCCS glass fibres [66,67]. They compared CCS circular fibres (KS161-454) with cocoon (peanut)-shaped (KSH081-870) and flat (oval) fibres (HISS4-454) obtained from Nittobo Glass Fibre Research Laboratory (presumably before the NCCS fibres were available commercially). All three fibre types were continuous; the cocoon-shaped fibres had a flatness ratio of about two and a CS area of 171 μm^2 , the flat fibre had a flatness of about four and a CS area of 125 μm^2 , and the CCS fibres had a CS area of about 131 μm^2 . These fibres were used to produce 68% fibre volume fraction UD epoxy laminates. Both the laminates containing both NCCS fibres were prone to preferred CS orientation during production, which resulted in large regions of fibre–fibre contact. These fibre contact areas acted as weak sites for delamination. Consequently, the Mode I, Mode II and ILSS tests all indicated a reduced delamination resistance for the NCCS composite systems compared with the CCS fibre composites.

A 1987 patent from Nittobo contains results on the mechanical properties of injection-moulded NCCS and CCS glass fibre reinforced thermoplastics [68]. The NCCS cocoon-shaped fibres had the equivalent CS area as the comparative 13 μm diameter CCS fibres. Data on acrylonitrile–styrene (SAN), acrylonitrile–butadiene–styrene (ABS), and polybutylene terephthalate (PBT) reinforced polymers were presented. The results for the tensile

strength over a 20–60 wt% fibre range are summarised in Figure 12. Although the NCCS composites also show some evidence of a tapering off of tensile strength increase at higher fibre content, it clearly is less strong than with CCS composites. This results in a significantly greater tensile strength being achievable at high fibre contents. Generally, there was no significant difference in the tensile modulus of these two types of composite reported. However, the improved reinforcement effect at high fibre contents was also quite pronounced in the unnotched impact data presented in this patent.

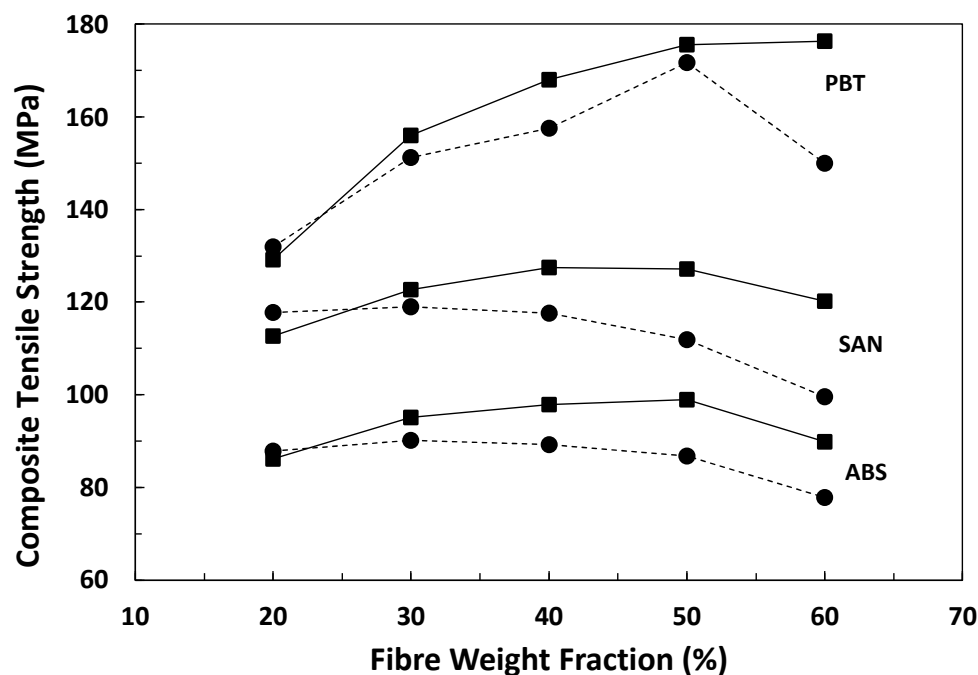


Figure 12. Tensile strength versus fibre weight fraction for various injection-moulded flat and circular fibre composites [68] (solid lines represent flat fibres, dashed lines represent circular fibres).

A 2006 patent from EMS Chemie AG discussed injection-moulded reinforced polyamide 12 (PA12) with flat glass fibres [69]. Data were presented in the examples for injection-moulded PA12 composites. Examples were presented of composites containing 50 wt% and 65 wt% fibres. The chopped fibres compared were a CCS reference sample, Bayer CS 7928, 10 μm diameter, and NCCS fibres Nittobo CSG3PA-820 with a flatness of four ($7 \times 28 \mu\text{m}$). Data were presented showing that the NCCS fibre (50 wt%, 65 wt%) containing composites have higher tensile strength (+9%, +16%), unnotched Charpy impact (+9%, +60%) and notched Charpy impact (+32%, +29%). The effect of fibre flatness on the properties of injection-moulded NCCS glass fibre reinforced polyamide 6T/6I was reported in a 2008 patent from EMS Chemie [70]. Data taken from that patent are plotted in Figure 13, which shows the mechanical performance of 60 wt% NCCS glass fibre polyamide relative to CCS reference samples. The two NCCS products from Nittobo had a flatness of two and four with a CS area of approximately $155 \mu\text{m}^2$. The 10 μm diameter CCS reference fibres were from Bayer with a CS area of approximately $78 \mu\text{m}^2$. It is known that the performance of CCS glass fibre reinforced polyamide increases with decreasing CS area [71,72]. Despite the much greater CS area of the flat fibres used in this example, it can be seen that the performance improves significantly with increasing fibre flatness.

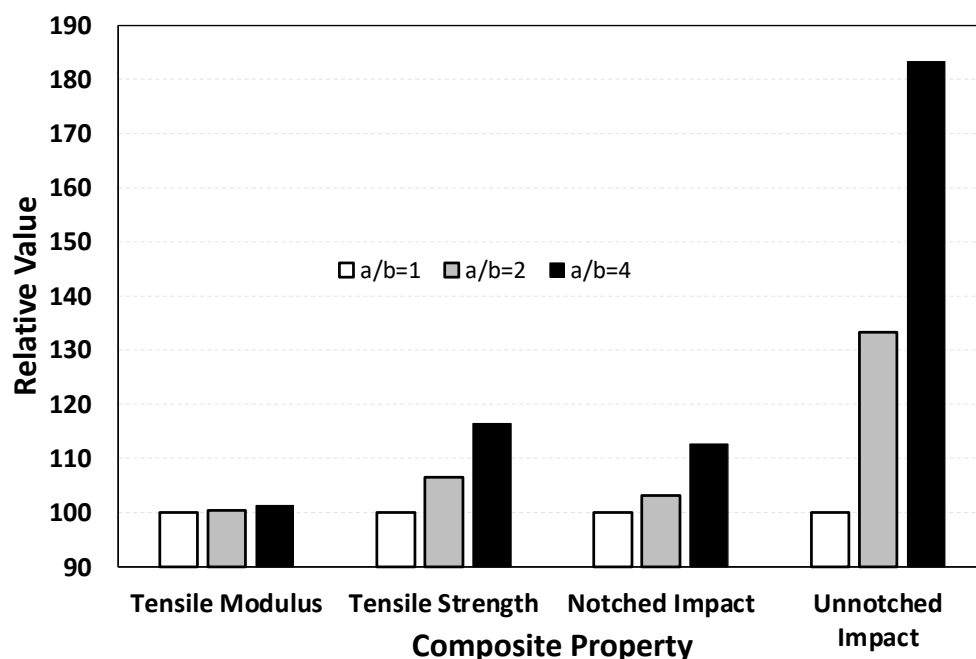


Figure 13. Comparison of tensile strength of injection-moulded fibre reinforced PA6,6 composites, with varying degrees of flatness [69].

Tanaka et al. compared circular and flat glass fibre performance of injection-moulded long fibre polypropylene (LFPP) composites [73]. The NCCS flat fibres, obtained from Nittobo, had a flatness value of four and a CS area equivalent to that of the CCS fibres with an average diameter of 17 μm . LFPP pellets were produced with a fibre content weight range of 20–50%. After injection moulding, it was noted that the flat fibre compounds delivered longer average residual fibre lengths in the moulded composites. Unnotched Charpy impact values obtained for flat fibre composites were consistently greater, especially at higher fibre contents where circular fibres exhibited sharply decreasing performance with increasing fibre content.

Heo et al. studied the performance of injection-moulded short fibre polyphenylene sulphide composites containing from 30 wt% to 70 wt% CCS circular or NCCS cocoon-shaped and flat glass fibres [74]. The glass fibres were provided by Nittobo. Flat fibres (CSG 3PA-830) had a flatness value of four, cocoon-shaped fibres (CSH 3PA-860S) had a flatness of about two, and both had a cross-section area equivalent to that of the 15 μm diameter circular fibres (CS 3J-953S). They found that the tensile strength of the cocoon fibre composites was marginally higher than the CCS fibre composites. However, the flat fibre composites had tensile strengths that were significantly greater across all fibre fractions investigated. The average residual fibre lengths in the moulded composites were consistently higher for both flatness NCCS fibre composites over the fibre content range of the study. Notched Izod impact performance was also consistently higher for both NCCS fibre composites, especially at higher fibre contents, where CCS fibre composites exhibited a decrease in impact performance with increasing fibre content. In another paper from the same institute, Kim et al. reported on the properties of injection-moulded glass fibre polyethylene terephthalate composites containing the same NCCS flat glass fibres [75,76]. They also reported higher composite tensile strength for the flat fibre composites over a range of fibre content. However, there were no significant differences in the impact performance measured for the flat and circular fibre reinforced composites.

A 2018 patent from BASF SE discussed injection-moulded reinforced high-temperature polyamide PA66/6T (and some blends) with flat glass fibres [77]. Examples were presented of composites containing fibre contents in the range of 17–70%. The chopped fibres compared were a CCS reference sample, NEG ECS 03T-289H, 10 μm diameter, and NCCS fibres

($7 \times 28 \mu\text{m}$). The data presented showed that the notched impact and tensile strength of the polyamide composites were increased by the use of the NCCS flat glass fibres instead of CCS normal fibres. This increase in performance of the flat fibre composites was particularly notable after the composites were exposed to moisture conditioning (14 days at 70°C and 62% RH). Interestingly, this could be correlated with the observation that the flat fibre composites were found to absorb significantly less moisture during conditioning compared to the CCS fibre composites. In another patent from BASF SE, the fatigue performance of injection-moulded glass reinforced polyamide PA66 is discussed [78]. The effects of two types of NCCS glass fibres (CPIC ESC301-HF with a flatness of four and Taishan T4355 with a flatness of three, $9 \times 27 \mu\text{m}$) were compared with the same CCS fibre reference (NEG ECS 03T-289H). Examples were given of composites containing 50 wt% and 60 wt% fibres. Prior to testing, the composite samples were conditioned at 70°C and an RH of 62%. It was stated that these conditions are equivalent to achieving an equilibrium moisture content at 23°C and 50% RH. The tensile strength differences between the various examples comparing flat and circular fibre were small and unlikely to be statistically different. However, the data presented on the fatigue resistance of the various examples showed very large improvements were possible when using flat fibre in place on traditional CCS fibres.

Bürenhaus and Moritzer recently reported on the reduction in fibre length during the compounding and moulding of glass reinforced thermoplastics [79]. The study included a comparison of CCS glass fibre (13 μm diameter) and an equivalent CS area NCCS flat fibre ($6 \times 22 \mu\text{m}$) in polyamide 6. They reported a small (+3.5%) increase in composite tensile strength for the flat fibres, which also correlated with a small increase in average residual fibre length in the moulding. All three suppliers of NCCS fibre products discuss the advantages of flat glass fibres in lowering the level of warpage in injection-moulded composite plates [3,62,80,81]. This difference in warpage is illustrated in Figure 14, showing the difference in warpage of injection-moulded plaques of 30% glass fibre reinforced PA 6,6 [82]. An example of the effect of NCCS flat glass fibre on the warpage of injection-moulded glass reinforced polycarbonate is discussed in a 2021 Nittobo patent [83]. The properties of composites produced with two NCCS glass fibre types with flatness values of four and six were compared across a range of fibre contents. Some differences in the warp of thin (0.4 mm) injection plates were observed between composites with the two different flatness ratio fibres. However, the reference CCS fibre plate had a warp of more than a factor 10 greater than the NCCS fibre composites.

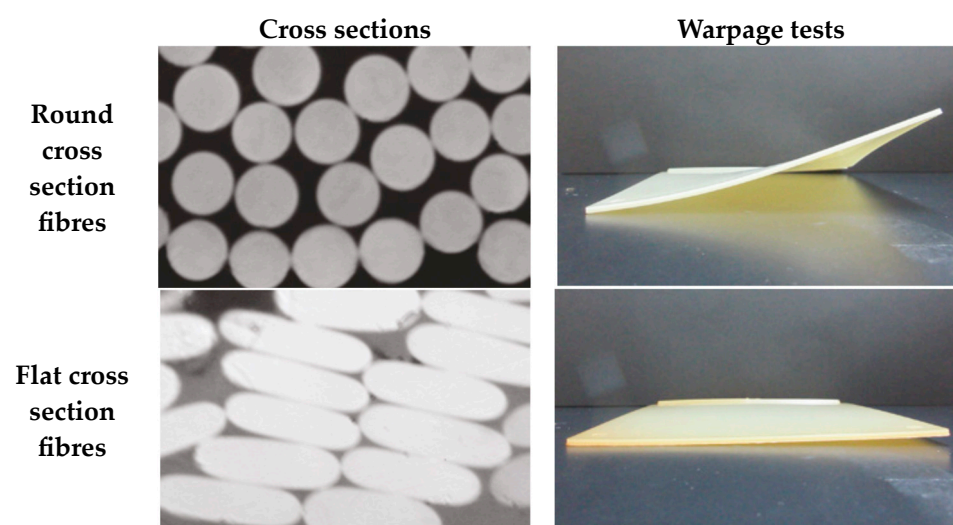


Figure 14. Images showing warpage in two edge-gated square test plaques (170 mm by 170 mm by 2.2 mm), moulded in PA66 30% reinforced with round and flat fibres, respectively [82].

Carlin et al. recently discussed some initial results from an extensive study of a comparison of the performance of flat and circular CS glass fibres and their injection-

moulded PA 6,6 composites [84]. Rovings of polyamide-compatible circular and flat E-glass fibres (2400 and 300 tex, respectively) were provided by NEG. Circular glass fibres supplied had a nominal 13-micron diameter, and flat glass fibres were of an equivalent cross-sectional area ($7 \times 28 \mu\text{m}$) with a flatness of four (see examples in Figure 15) [85]. NEG also supplied injection-moulded glass fibre reinforced PA 6,6 with fibre different weight fractions in the range of 30–55 wt%.

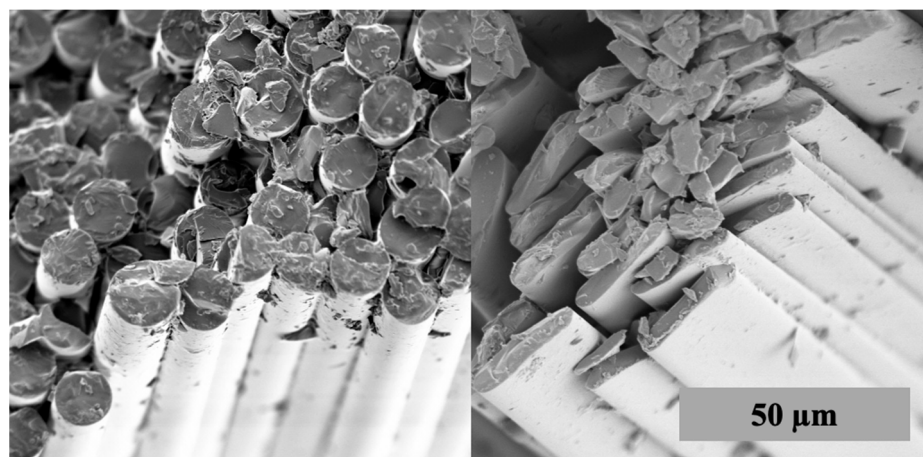


Figure 15. SEM of circular and flat cross-section glass fibres [85].

All glass fibres in the study were sized with the same polyamide-compatible sizing. In reporting the results of single fibre strength testing, it was noted that the measurement of accurate fibre CS is required and that this is more challenging with NCCS fibres. The results for the tensile strength of the PA 6,6 composites (dry and after 24 h boil conditioning) are reproduced in Figure 16. It can be seen that, compared to standard circular CS fibres, the flat fibres give composites with higher tensile strength at higher glass contents and also lower strengths at low fibre contents. These differences appear to be magnified after moisture conditioning. It was reported that flat fibre compounds also had a greater residual fibre length across the range of weight fractions. It was suggested that this could be due to the reduction in the second moment of area of the flat fibre, which would tend to increase fibre flexibility and reduce instances of fibre breakage during processing.

The available data where the influence of commercial NCCS glass fibres on the tensile performance of various injection-moulded thermoplastic composites is directly compared with an equivalent CCS fibre is summarised in Figure 17 [59,68–70,84]. This Figure shows the direct ratio in composite tensile strength obtained when comparing NCCS fibres (flatness range 2–4) to CCS fibres in the same matrix. It can be seen that there exists a clear trend for an increase in this ratio as the glass fibre content is increased. Interestingly, it appears that there is also a consistent trend for the CCS fibres to give slightly better performance at lower fibre contents, below about 30 wt%. Thomason has recently published the results of an analytical modelling study of this phenomenon, its influence on the critical fibre length in a discontinuous composite system, and the resulting effects on tensile strength in different thermoplastic matrix composites [85,86]. It was observed that, for fibres with the same CS area, CCS fibres have the minimum surface area. This means that the interfacial area in a composite is also a minimum. Consequently, at equal applied stress to the composite, the interfacial stress is higher for CCS fibres compared to NCCS fibres. This effect becomes greater as the flatness of the NCCS fibre is increased. Analytical modelling showed that this effect could result in an increasing NCCS:CCS composite tensile strength ratio as the fibre content of the composites is increased. The magnitude of this ratio predicted by the modelling was of the same order of magnitude as that observed in Figure 17. Thomason also extended the use of the model to include the effect of surface roughness and non-circularity observed in nearly all natural fibres, and many carbon fibres [85].

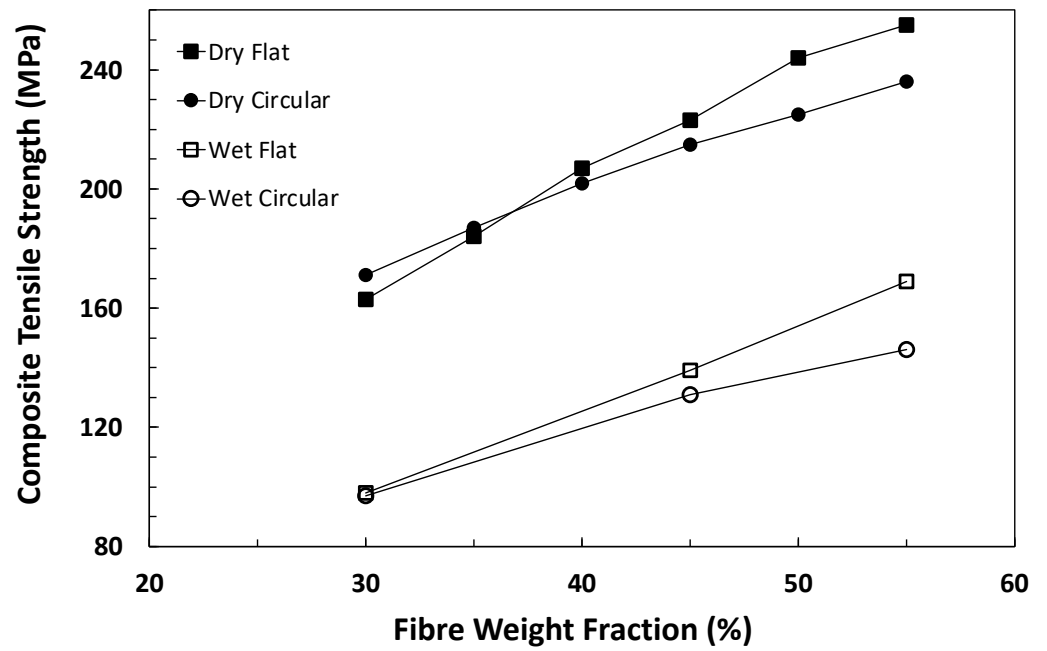


Figure 16. Comparison of tensile strength of injection-moulded flat and circular fibre PA6,6 composites [84].

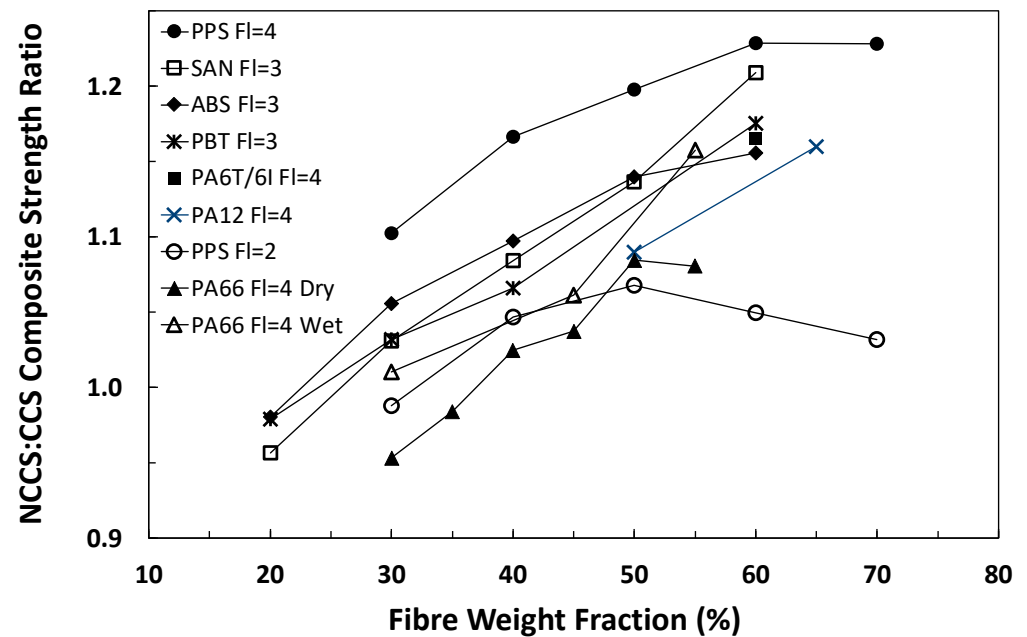


Figure 17. Ratio of tensile strength of NCCS:CCS glass fibre reinforced thermoplastics [59,68–70,84].

5. Conclusions

Despite mass-produced NCCS glass fibres only recently becoming available, the investigations of glass fibre CS shape date back to the early 1960s. Much of the early work was carried out on fibres produced individually using production technology similar to that used for optical fibre drawing. Most of this early work focussed on the preparation and characterisation of continuous fibre reinforced composites. This work clearly indicated that NCCS glass fibres offer a number of potential advantages over CCS glass fibres. A summary of the findings of this review on the potential advantages that NCCS glass fibres may bring to composite performance is given in Table 1. These include higher maximum fibre packing densities, improved composite transverse and compression performance, higher creep resis-

tance, increased resistance to fluid permeation, and improved vibration damping. Many of these experimental conclusions were supported by the results of modelling investigations. However, many of these early investigations also highlighted the technical challenges in producing NCCS glass fibres, particularly using the E-glass formulation, which is currently used in more than 90% of glass fibre reinforcement mass production.

Table 1. Summary of the differences in composite properties containing NCCS vs. CCS glass fibres.

Using ribbon glass fibres in UD composites
Increased in-plane transverse stiffness [8,9]
Improved creep resistance [12]
Fluid permeability reduction [10,14]
Increased modulus and strength [14,18,20]
Very high glass volume fractions are possible [14,18]
Using experimental fibre cross-section shapes in UD Composites
Elliptical fibres gave higher transverse stiffness [15]
Triangular fibres gave higher transverse stiffness [21]
Triangular fibres gave higher compressive and tensile strength [22]
Triangular fibres gave higher flexural strength and modulus [24]
Lobular fibres improved vibration damping [31–33]
Lobular fibres gave higher transverse modulus and strength [34]
Using commercial flat glass fibres in injection-moulded thermoplastic composites
Higher mechanical properties, especially at higher fibre content [68–72,74–77,84]
LFT-PP Improved impact [73]
Improved fatigue performance obtained in GF-PA [78]
Significant warpage reduction [2,27,28,80–82,87]
Lower interface stress leading to higher composite strength [85,86]

Consequently, the availability of mass-produced NCCS glass fibres required the glass fibre industry to tackle a number of issues in order to be able to manufacture such fibres in a cost-effective manner. The patent literature reveals that this has been achieved, to a certain extent, by a number of developments in glass fibre production technology. These include limiting the CS shape to relatively simple forms, which appear to be mainly variations in ribbon-type fibres. The fibre process developments to enable NCCS glass fibre production have involved glass melt viscosity control, bushing tip design and increased fibre cooling to maintain the NCCS shape. However, it seems likely that the mass production of NCCS fibres has not yet reached the levels of process efficiency of CCS glass fibres. Consequently, the cost of production of NCCS glass fibres may still significantly exceed that of CCS fibres.

Studies published in the patent and journal literature indicate that when mass-produced NCCS flat glass fibres are used to reinforce injection-moulded thermoplastic composites, significant reductions in the warpage of the composites can be achieved in comparison to normal CCS glass fibres. A limited amount of patent data indicates that fatigue resistance can be improved using NCCS flat glass fibre in place of traditional CCS fibres. However, there is clear evidence in many of the reviewed studies indicating that, as composite fibre content is increased, the NCCS flat fibre composites have increasingly better mechanical performance, particularly strength and impact, compared to CCS fibre composites. There also appears to be a generally accepted explanation that this increase in composite mechanical performance is related to the increased interfacial area in NCCS glass fibre composites. At any particular composite applied load, this increased interfacial area lowers interfacial stress, and hence, higher external loading is required to achieve interface and composite failure.

6. Future Perspectives

It is clear that NCCS glass fibres have the potential to generate composites with increased performance in some areas and may also permit tailoring of composite performance

to enable new applications to be developed. However, it has also been observed in this review that many of these composite performance improvements have been documented over 50 years ago, and it has been concluded that an important factor in the slow development of these ideas has been the technical and economic challenges faced by glass fibre producers to make NCCS glass fibres available on a commercial scale. To date, the only main application which has been opened up appears to be in thin-walled injection moulding, where the significantly lower composite warpage performance given by chopped flat fibres is utilised.

On considering the content of this review, largely summarised in Table 1, it is relatively easy to envisage a number of large composite applications which might benefit from the use of NCCS glass fibres. However, many of these possibilities would require the availability of continuous fibre products, probably in combination with some modification of composite production methods to enable control of the rotational orientation of the NCCS fibres along their length. It would, therefore, appear that the future development of NCCS glass fibre technology is firmly in the hands of the glass fibre manufacturing companies and depends on their interest, willingness, and technical ability to support breakthrough research and development in this area of composite science.

Supplementary Materials: The following supporting information can be downloaded at: <https://www.mdpi.com/article/10.3390/fib12110098/s1>, Tables S1–S5: NCCS Glass Fibre Patents.

Author Contributions: Conceptualisation, J.T. and L.Y.; methodology, J.T.; validation, J.T.; formal analysis, A.C. and J.T.; investigation, A.C. and J.T.; resources, L.Y. and J.T.; writing—original draft preparation, J.T.; writing—review and editing, J.T. and A.C.; visualisation, J.T.; supervision, J.T. and L.Y.; project administration, L.Y. and J.T.; funding acquisition, J.T. and L.Y. All authors have read and agreed to the published version of the manuscript.

Funding: One of the authors (A.C.) received funding support from Nippon Electric Glass and the International Strategic Partnership Fund of the University of Strathclyde.

Data Availability Statement: No new data were created or analysed in the preparation of this review. Data sharing is not applicable to this article.

Acknowledgments: The authors are grateful to Q. Chouffart for supplying Figure 9.

Conflicts of Interest: The authors declare no conflicts of interest. The funders had no role in the design of the study; in the collection, analyses, or interpretation of data; in the writing of the manuscript; or in the decision to publish the results.

References

1. Zu, Q.; Solvang, M.; Li, H. Commercial Glass Fibers. In *Fiberglass Science and Technology Chemistry, Characterization, Processing, Modeling, Application, and Sustainability*; Li, H., Ed.; Springer International Publishing: Cham, Switzerland, 2021.
2. Nittobo Flat Fibers Center. Available online: <https://polymer-additives.specialchem.com/centers/nittobo-flat-glass-fibers> (accessed on 13 September 2024).
3. Moore, S. Flat Glass Fiber Developed for Reinforcement of Thermoplastic Resins. Available online: <https://www.plasticstoday.com/materials/flat-glass-fiber-developed-for-reinforcement-of-thermoplastic-resins> (accessed on 13 September 2024).
4. CPIC Develops Family of Unique Fiberglass Products. Available online: <https://www.compositesworld.com/news/cpic-develops-family-of-unique-fiberglass-products> (accessed on 13 September 2024).
5. Ennis, B.L.; Perez, H.S.; Norris, R.E. Identification of the optimal carbon fiber shape for cost-specific compressive performance. *Mater. Today Commun.* **2022**, *33*, 104298. [CrossRef]
6. Thomason, J.; Carruthers, J.; Kelly, J.; Johnson, G. Fibre cross-section determination and variability in sisal and flax and its effects on fibre performance characterisation. *Compos. Sci. Technol.* **2011**, *71*, 1008–1015. [CrossRef]
7. Thomason, J.L.; Carruthers, J. Natural fibre cross sectional area, its variability and effects on the determination of fibre properties. *J. Biobased Mater. Bioenergy* **2012**, *6*, 424–430. [CrossRef]
8. Halpin, J.C.; Thomas, R.L. Ribbon Reinforcement of Composites. *J. Compos. Mater.* **1968**, *2*, 488–497. [CrossRef]
9. Lim, T.C. Simplified Transverse Young's Modulus of Aligned Ribbon-Reinforced Composites by the Mechanics-of-Materials Approach. *J. Reinf. Plast. Compos.* **2003**, *22*, 257–269. [CrossRef]
10. Brydges, W.T.; Gulati, S.T.; Baum, G. Permeability of glass ribbon-reinforced composites. *J. Mater. Sci.* **1975**, *10*, 2044–2049. [CrossRef]

11. Gulati, S.T. Longitudinal and transverse strength of glass ribbon for plastic reinforcement. *J. Mater. Sci.* **1976**, *11*, 631–637. [[CrossRef](#)]
12. Li, J.; Weng, G. Effective creep behavior and complex moduli of fiber- and ribbon-reinforced polymer-matrix composites. *Compos. Sci. Technol.* **1994**, *52*, 615–629. [[CrossRef](#)]
13. Li, J.; Weng, G.J. Stress-strain relations of a viscoelastic composite reinforced with elliptic cylinders. *J. Thermoplast. Compos. Mater.* **1997**, *10*, 19–30. [[CrossRef](#)]
14. Rexer, J.; Anderson, E. Composites with planar reinforcements (flakes, ribbons)—A review. *Polym. Eng. Sci.* **1979**, *19*, 1–11. [[CrossRef](#)]
15. Rosen, B.W.; Dow, N.F.; Hashin, Z. Mechanical Properties of Composites. NASA CR-31. April 1964. Available online: <https://apps.dtic.mil/sti/tr/pdf/ADA308219.pdf> (accessed on 16 August 2024).
16. Eakins, W.J.; Humphrey, R.A. Studies of Hollow Multipartitioned Ceramic Structures. NASA CR-142. December 1964. Available online: <https://ntrs.nasa.gov/citations/19650003209> (accessed on 18 August 2024).
17. Humphrey, R.A. Feasibility Study on Hexagonal Glass Filaments. Final Report Office of Naval Research Contract Nonr-3885(00)(X) June 1963. Available online: <https://apps.dtic.mil/sti/citations/AD0407554> (accessed on 18 August 2024).
18. Humphrey, R.A. Precision Winding of Cylindrical Composites with Shaped Glass Filaments. NASA CR-517. August 1966. Available online: <https://ntrs.nasa.gov/citations/19660023668> (accessed on 18 August 2024).
19. Humphrey, R.A. Preparation of Filament Wound Glass Microtape Research Specimens. NASA CR-72459. July 1968. Available online: <https://ntrs.nasa.gov/citations/19680026243> (accessed on 18 August 2024).
20. Humphrey, R.A. Shaped Glass Fibers. In *Modern Composite Materials*; Broutman, L.J., Krock, P.R., Eds.; Addison-Wesley: Boston, MA, USA, 1967.
21. Dow, N.F. Enhancement of the Transverse Properties of Fibrous Composites. CR-78307. February 1966. Available online: <https://www.fid-move.de/en/search/id/ntis:9389d3553630d4e8b4372aa2efdc2632dfcf4807/Enhancement-of-the-Transverse-Properties-of-Fibrous?cHash=a533301bc9e00074eb90c05768fac9d8> (accessed on 18 August 2024).
22. Bond, I.; Hucker, M.; Weaver, P.; Bleay, S.; Haq, S. Mechanical behaviour of circular and triangular glass fibres and their composites. *Compos. Sci. Technol.* **2002**, *62*, 1051–1061. [[CrossRef](#)]
23. Robati, H.; Attar, M.M. Analytical study of a pin-loaded hole in unidirectional laminated composites with triangular and circular fibers. *J. Appl. Mech.* **2013**, *80*, 021018–210187. [[CrossRef](#)] [[PubMed](#)]
24. Liu, X.; Wang, R.; Wu, Z.; Liu, W. The effect of triangle-shape carbon fiber on the flexural properties of the carbon fiber reinforced plastics. *Mater. Lett.* **2012**, *73*, 21–23. [[CrossRef](#)]
25. Yang, L.; Liu, X.; Wu, Z.; Wang, R. Effects of triangle-shape fiber on the transverse mechanical properties of unidirectional carbon fiber reinforced plastics. *Compos. Struct.* **2016**, *152*, 617–625. [[CrossRef](#)]
26. Gallucci, R.; Naar, R.; Liu, H.I.; Mordecai, W.; Yates, J.; Huey, L.; Schweizer, R. Reducing warp in thermoplastics with bilobe glass fibers. *Plast. Eng.* **1993**, *49*, 23–25.
27. Huey, L.J. Method and Apparatus for Making Tapered Mineral and Organic Fibers. U.S. Patent 4,666,485, 19 May 1987.
28. Huey, L.J.; Beuther, P.D. Method and Apparatus for Making Non-Circular Mineral Fibers. U.S. Patent 4,636,234, 13 January 1987.
29. Harris, J.; Bond, I.; Weaver, P.; Wisnom, M.R. Improving through-thickness properties of fibre reinforced plastics using novel shaped fibres. *Proc. Inst. Mech. Eng. Part L J. Mater. Des. Appl.* **2004**, *218*, 29–35. [[CrossRef](#)]
30. Harris, J.; Bond, I.; Weaver, P.; Wisnom, M.; Rezai, A. Measuring strain energy release rate (G_{IC}) in novel fibre shape composites. *Compos. Sci. Technol.* **2006**, *66*, 1239–1247. [[CrossRef](#)]
31. Agnese, F.; Scarpa, F. Damping properties of star-shaped biphase macro-composites. January 2012. Available online: https://www.academia.edu/download/42580807/Macro_composites_with_non-classical_Incl20160211-12036-17wypoi.pdf (accessed on 17 March 2024).
32. Agnese, F.; Scarpa, F. Macro composites with non-classical inclusions for vibration damping in wind turbine. In *Active and Passive Smart Structures and Integrated Systems*; SPIE: Cergy Pontoise, France, 2012; Volume 8341, pp. 94–104.
33. Agnese, F.; Scarpa, F. Macro-composites with star-shaped inclusions for vibration damping in wind turbine blades. *Compos. Struct.* **2014**, *108*, 978–986. [[CrossRef](#)]
34. Yang, L.; Li, Z.; Sun, T.; Wu, Z. Effects of gear-shape fibre on the transverse mechanical properties of unidirectional composites: Virtual material design by computational micromechanics. *Appl. Compos. Mater.* **2017**, *24*, 1165–1178. [[CrossRef](#)]
35. Reichanadter, A.; Mansson, J.A. Extending the Gutowski model to kidney-bean and elliptically shaped fibers. *J. Compos. Mater.* **2022**, *56*, 1313–1318. [[CrossRef](#)]
36. Reichanadter, A.; Mansson, J.-A.E. Permeability simulation of kidney-bean shaped carbon fibers. *Mater. Today Commun.* **2022**, *31*, 103385. [[CrossRef](#)]
37. Hanhan, I.; Sangid, M.D. Design of Low Cost Carbon Fiber Composites via Examining the Micromechanical Stress Distributions in A42 Bean-Shaped versus T650 Circular Fibers. *J. Compos. Sci.* **2021**, *5*, 294. [[CrossRef](#)]
38. Xu, Z.; Li, J.; Wu, X.; Huang, Y.; Chen, L.; Zhang, G. Effect of kidney-type and circular cross sections on carbon fiber surface and composite interface. *Compos. Part A Appl. Sci. Manuf.* **2008**, *39*, 301–307. [[CrossRef](#)]
39. Xu, Z.; Huang, Y.; Liu, L.; Zhang, C.; Long, J.; He, J.; Shao, L. Surface characteristics of kidney and circular section carbon fibers and mechanical behavior of composites. *Mater. Chem. Phys.* **2007**, *106*, 16–21. [[CrossRef](#)]

40. Clarke, R.J.; Miller, D.A.; Cairns, D.S. Effect of fiber shape on defect sensitivity of fiber kinking for pultruded carbon fiber composites. In Proceedings of the International SAMPE Technical Conference, Virtual Event, 29 June–1 July 2021; pp. 1211–1222.
41. Kitagawa, Y.; Yoshimura, A.; Arai, M.; Goto, K.; Sugiura, N. Experimental and numerical evaluation of effects of kidney-shape carbon fiber on transverse cracking of carbon fiber reinforced plastics. *Compos. Part A Appl. Sci. Manuf.* **2022**, *152*, 106690. [[CrossRef](#)]
42. Higuchi, R.; Yokozeki, T.; Nagashima, T.; Aoki, T. Evaluation of mechanical properties of noncircular carbon fiber reinforced plastics by using XFEM-based computational micromechanics. *Compos. Part A Appl. Sci. Manuf.* **2019**, *126*. [[CrossRef](#)]
43. Camarena, E.; Clarke, R.J.; Ennis, B.L. Compressive strength improvements from noncircular carbon fibers: A numerical study. *Compos. Sci. Technol.* **2023**, *242*, 110168. [[CrossRef](#)]
44. Wang, M.; Hang, X. Effects of microstructure characteristics on the transverse moisture diffusivity of unidirectional composite. *Sci. Eng. Compos. Mater.* **2023**, *30*, 20220201. [[CrossRef](#)]
45. He, C.; Ge, J.; Cao, X.; Chen, Y.; Chen, H.; Fang, D. The effects of fiber radius and fiber shape deviations and of matrix void content on the strengths and failure mechanisms of UD composites by computational micromechanics. *Compos. Sci. Technol.* **2021**, *218*, 109139. [[CrossRef](#)]
46. Wallenberger, F.T.; Watson, J.C.; Li, H. Glass fibers. In *Composites, ASM Handbook*; Miracle, D.B., Donaldson, S.L., Eds.; ASM International: Novelt, OH, USA, 2001; Volume 21.
47. Thomason, J.L. Glass Fibre Sizing: A Review of Size Formulation Patents. Blurb Incorporated 2015. Available online: <http://www.blurb.co.uk/b/6244662-glass-fibre-sizing> (accessed on 12 September 2024).
48. Thomason, J.L. Glass fibre sizing: A review. *Compos. Part A Appl. Sci. Manuf.* **2019**, *127*, 105619. [[CrossRef](#)]
49. Chouffart, Q.; Simon, P.; Terrapon, V.E. Numerical and experimental study of the glass flow and heat transfer in the continuous glass fiber drawing process. *J. Mech. Work. Technol.* **2016**, *231*, 75–88. [[CrossRef](#)]
50. Chouffart, Q. Experimental and Numerical Investigation of the Continuous Glass Fiber Drawing Process. Ph.D. Thesis, University of Liege, Liege, Belgium, 2018.
51. Thomason, J.; Nagel, U.; Yang, L.; Sáez, E. Regenerating the strength of thermally recycled glass fibres using hot sodium hydroxide. *Compos. Part A Appl. Sci. Manuf.* **2016**, *87*, 220–227. [[CrossRef](#)]
52. Yue, Y.; Zheng, Q. Fiber spinnability of glass melts. *Int. J. Appl. Glass Sci.* **2017**, *8*, 37–47. [[CrossRef](#)]
53. Kraxner, J.; Liška, M.; Klement, R.; Chromčíková, M. Surface tension of borosilicate melts with the composition close to the E-glass. *Ceram. Silik.* **2009**, *53*, 141–143.
54. Jensen, T.H. A Novel Fiber-Forming Bushing and Tip Plate. U.S. Patent 4,941,903, 17 July 1990.
55. Jensen, T.H. Method and Apparatus for Forming Round Glass Fibers. U.S. Patent 5,062,876, 5 November 1991.
56. Warthen, W.P. Attenuated Mineral Filaments. U.S. Patent 3,231,459, 25 January 1966.
57. Russell, R.G. Method and Apparatus for Forming Fibers. U.S. Patent 4,144,044, 13 March 1979.
58. Huang, J. Method of Making Shaped Fibers. U.S. Patent 5,776,223, 7 July 1998.
59. Wright, R.F.; Boudreaux, E. Polymer/Bi-Lobal Fiber Composites Having Improved Strength. U.S. Patent 5,250,603, 5 October 1993.
60. Nittobo Company History. Available online: <https://www.nittobo.co.jp/eng/corporate/atag glance/100th.htm> (accessed on 13 September 2024).
61. Shioura, K.; Yamazaki, S.; Shono, H. Method for Producing Glass Fibers Having Non-Circular Cross Sections. U.S. Patent 4,698,083, 6 October 1987.
62. JEC Press Release 2 March 2011. Available online: <https://pieweb.plasteurope.com/members/pdf/p218820c.PDF> (accessed on 14 September 2024).
63. Imaizumi, H.; Yamanaka, Y.; Morimoto, K. Fiber-Reinforced Thermoplastic Resin Molded Article. U.S. Patent 7,858,172, 28 December 2010.
64. Taguchi, H.; Shioura, K.; Sugeno, M. Nozzle tip For Spinning Glass Fiber Having Deformed Cross-Section and a Plurality of Projections. U.S. Patent 5,462,571, 31 October 1995.
65. Konno, M.; Miura, Y.; Saito, S.; Kasai, S. Glass Fiber Nonwoven Fabric and Printed Wiring Board. U.S. Patent 6,543,258, 8 April 2003.
66. Deng, S.; Ye, L.; Mai, Y.-W. Influence of fibre cross-sectional aspect ratio on mechanical properties of glass fibre/epoxy composites I. Tensile and flexure behaviour. *Compos. Sci. Technol.* **1999**, *59*, 1331–1339. [[CrossRef](#)]
67. Deng, S.; Ye, L.; Mai, Y.-W. Influence of fibre cross-sectional aspect ratio on mechanical properties of glass-fibre/epoxy composites II. Interlaminar fracture and impact behaviour. *Compos. Sci. Technol.* **1999**, *59*, 1725–1734. [[CrossRef](#)]
68. Koike, R.; Shioura, K.; Shimanuki, S. Glass-Fiber Reinforced Resin Molded Articles and a Method for Producing the Same. E.P. 0246620, 19 May 1987.
69. Stöppelmann, G.; Rexin, O.; Eichhorn, V. Polyamide Moulding Materials Reinforced with Flat Glass Fibers and Articles Injection-Moulded Therefrom. E.P. 1942147, 28 December 2006.
70. Harder, P.; Jeltsch, T.; Lamberts, N. High-Temperature Polyamide Molding Compounds Reinforced with Flat Glass Fibers. U.S. Patent 8,324,307, 4 December 2012.
71. Thomason, J. The influence of fibre properties of the performance of glass-fibre-reinforced polyamide 6,6. *Compos. Sci. Technol.* **1999**, *59*, 2315–2328. [[CrossRef](#)]

72. Thomason, J.L. Structure–property relationships in glass reinforced polyamide, part 2: The effects of average fiber diameter and diameter distribution. *Polym. Compos.* **2007**, *28*, 331–343. [[CrossRef](#)]
73. Tanaka, K.; Katayama, T.; Tanaka, T.; Anguri, A. Injection Molding of Flat Glass Fiber Reinforced Thermoplastics. *Int. J. Mod. Phys. B* **2010**, *24*, 2555–2560. [[CrossRef](#)]
74. Heo, K.Y.; Park, S.M.; Lee, E.S.; Kim, M.S.; Sim, J.H.; Bae, J.S. A study on properties of the glass fiber reinforced PPS composites for automotive headlight source module. *Compos. Res.* **2016**, *29*, 293–298. [[CrossRef](#)]
75. Kim, J.H.; Lee, E.S.; Kim, M.S.; Sim, J.H. Mechanical characteristics of gf/recycled PET thermoplastic composites with chopped fiber according to cross section. *Text. Color. Finish.* **2017**, *29*, 239–246.
76. Sim, J.-H.; Yu, S.-H.; Yoon, H.-S.; Kwon, D.-J.; Lee, D.-H.; Bae, J.-S. Characteristic evaluation and finite element analysis of glass fiber/recycled polyester thermoplastic composites by cross-sectional shape of glass fiber. *Compos. Part B Eng.* **2021**, *223*, 109095. [[CrossRef](#)]
77. Kim, T.Y. Polyamide Formulations Comprising Semi-Crystalline Copolyamide and Flat Glass Fibers. U.S. Patent 11,555,117, 17 January 2023.
78. Robert, G.; Kim, T.Y.; Wang, W.; Speroni, F. Polyamide Composition Containing Flat Glass Fibres with Improved Fatigue Resistance. U.S. Patent 11,920,034, 5 March 2024.
79. Bürenhaus, F.; Moritzer, E. Influence of fiber geometry and sizing on glass fiber breakage. In *AIP Conference Proceedings*; AIP Publishing: Melville, NY, USA, 2023; Volume 2607.
80. Nittobo Flat Fibers Centre. Available online: <https://polymer-additives.specialchem.com/centers/nittobo-flat-glass-fibers/main-features> (accessed on 14 September 2024).
81. Sherman, L.S. Novel ‘Flat’ Fiberglass Enhances Injection Molded TP Composites. Available online: <https://www.ptonline.com/articles/novel-flat-fiberglass-enhances-injection-molded-tp-composites> (accessed on 14 September 2024).
82. Mapleston, P. Reinforcing Options for Compounders. *Compounding World*, October 2018; pp. 77–84. Available online: <https://content.yudu.com/web/1rl19/0A1rl2p/CWOct18/html/index.html?page=78&origin=reader> (accessed on 15 September 2024).
83. Nukui, Y.; Sasamoto, T. Glass-Fiber-Reinforced Resin Plate. U.S. Patent Application 2023/0118488, 20 April 2023.
84. Carlin, A.; Yang, L.; Thomason, J.L. An investigation into flat glass fibres for injection moulded polyamide 6,6 composites. Paper 193. In *Proceedings of the 23rd International Conference on Composite Materials*, Belfast, UK, 30 July–4 August 2023.
85. Thomason, J. The influence of fibre cross section shape and fibre surface roughness on composite micromechanics. *Micro* **2023**, *3*, 353–368. [[CrossRef](#)]
86. Thomason, J.L. Flat glass fibres: The influence of fibre cross section shape on composite micromechanics and composite strength. *Compos. Part A Appl. Sci. Manuf.* **2023**, *169*, 107503. [[CrossRef](#)]
87. Bregar, B. Flat Fiberglass Offers Higher Loading and Lower Warpage in Thin-Wall Parts. Available online: <https://www.plasticsnews.com/article/20180221/NEWS/180229979> (accessed on 1 November 2024).

Disclaimer/Publisher’s Note: The statements, opinions and data contained in all publications are solely those of the individual author(s) and contributor(s) and not of MDPI and/or the editor(s). MDPI and/or the editor(s) disclaim responsibility for any injury to people or property resulting from any ideas, methods, instructions or products referred to in the content.